



## VERIFICATION

I, Motoo AKAGI, a national of Japan, Nitto IPO Ltd., No.17 Arai Bldg., 3-3, Shinkawa 1-chome, Chuo-ku, Tokyo 104-0033, Japan, verify that to the best of my knowledge and belief the following is a true translation made by me of the annexed document which is Japanese Patent Application, No. 2001-271770 filed on September 7, 2001.

Dated 28th day of June, 2004

Motoo Akagi

Motoo AKAGI, Translator

[Document Name] Application for Patent

[Reference No.] NT01P0429

[Application Date] September 7, 2001

[Destination] Commissioner, Patent Office

[International Patent Classification] G11B 5/66

[Inventor]

[Address] 2880 Kozu, Odawara-shi, Kanagawa-ken,  
256-8510 Japan  
Hitachi, Ltd.,  
Data Storage Systems Division  
[Name] Tetsuya KANBE

[Inventor]

[Address] 2880 Kozu, Odawara-shi, Kanagawa-ken,  
256-8510 Japan  
Hitachi, Ltd.,  
Data Storage Systems Division  
[Name] Hiroyuki SUZUKI

[Inventor]

[Address] 2880 Kozu, Odawara-shi, Kanagawa-ken,  
256-8510 Japan  
Hitachi, Ltd.,  
Data Storage Systems Division  
[Name] Yotsuo YAHISA

[Inventor]

[Address] 280, 1-chome, Higashi-koigakubo,  
Kokubunji-shi, Tokyo  
Hitachi, Ltd.,  
Central Research Laboratory  
[Name] Yoshiyuki HIRAYAMA

[Inventor]

[Address] 2880 Kozu, Odawara-shi, Kanagawa-ken,  
256-8510 Japan  
Hitachi, Ltd.,  
Data Storage Systems Division

[Name] Hidekazu KASHIWASE

[Applicant for Patent]

[Identification No.] 000005108  
[Name] Hitachi, Ltd.

[Agent]

[Identification No.] 100068504  
[Patent Attorney] Katsuo OGAWA  
[Telephone No.] 03-3661-0071

[Agent]

[Identification No.] 100086656  
[Patent Attorney] Kyousuke TANAKA  
[Telephone No.] 03-3661-0071

[Agent]

[Identification No.] 100094352  
[Patent Attorney] Ko SASAKI  
[Telephone No.] 03-3661-0071

[Designation of Charge]

[Ledger No. for Prepayment] 081423  
[Amount of Payment] 21000

[List of Document Submitted]

[Object Name]	Specification	01
[Object Name]	Drawings	01
[Object Name]	Abstract	01

[Proof] Required



[Type of the Document] Specification

[Title of the Invention]

MAGNETIC RECORDING MEDIUM AND MAGNETIC RECORDING  
APPARATUS

5 [What is claimed is]

[Claim 1]

A longitudinal magnetic recording medium characterized in that a magnetic layer is formed on a non-magnetic substrate via a plurality of underlayers, 10 the magnetic layer comprises a lower magnetic layer containing at least one of Ru or Re in an amount of not less than 3 at% to not more than 30 at%, and Cr in an amount of not less than 0 at% to not more than 18 at%, and further containing at least one of B or C in an 15 amount of not less than 0 at% to not more than 20 at%, and the balance being made up of Co, and an upper magnetic layer containing Co as a main component, anti-ferromagnetically coupled with the lower magnetic layer via a non-magnetic intermediate layer.

20 [Claim 2]

The longitudinal magnetic recording medium according to claim 1 characterized in that the plurality of the underlayers comprise a non-magnetic and amorphous structured first underlayer containing Co 25 or Ni as a main component, and a body-centered cubic structured second underlayer containing Cr.

[Claim 3]

The longitudinal magnetic recording medium

according to claim 1 characterized in that the plurality of the underlayers comprise a first underlayer having a B2 structure, and a body-centered cubic structured second underlayer containing Cr.

5 [Claim 4]

The longitudinal magnetic recording medium according to claim 1 characterized in that at least one layer of the plurality of the underlayers is made of a non-magnetic and hexagonal close-packed structured 10 alloy material containing Co.

[Claim 5]

The longitudinal magnetic recording medium according to claim 4 characterized in that the underlayer made of the non-magnetic and hexagonal 15 close-packed structured alloy material containing Co is formed between the lower magnetic layer and the second underlayer.

[Claim 6]

The longitudinal magnetic recording medium 20 according to claim 4 or claim 5 characterized in that the underlayer made of the non-magnetic and hexagonal close-packed structured alloy material containing Co is made of a Co-Ru alloy containing Ru in an amount of not less than 35 at% to not more than 60 at%.

25 [Claim 7]

The longitudinal magnetic recording medium according to any one of claims 1 to 6 characterized in that at least one layer of the plurality of the

underlayers is made of a body-centered cubic structured alloy material containing Cr, and the Cr alloy contains B in an amount of not less than 2 at% to not more than 15 at%.

5 [Claim 8]

A magnetic storage apparatus, comprising: a magnetic recording medium; a driver for driving it in the recording direction; a composite head having an inductive magnetic head for recording and a spin-valve type magnetic head for reading in combination; means for causing the head to perform relative movement with respect to the medium; and a read / write signal processing means with respect to the head, the magnetic recording medium being constituted by the longitudinal magnetic recording medium according to any one of claims 1 to 7.

[Detailed Description of the Invention]

[0001]

[Field of the Invention]

20 The present invention relates to a magnetic recording medium and a magnetic storage apparatus. More particularly, it relates to a technology of a longitudinal magnetic recording medium which has a low noise and a high coercivity, and is also sufficiently stable against thermal fluctuation. Further, it relates to a technology of a high reliability magnetic storage apparatus having an areal recording density of 25 50 megabits per square millimeter or more, which has

been implemented by combining the longitudinal magnetic recording medium technology with a technology of a high sensitivity magnetic head, and optimizing the read / write conditions.

5 [0002]

[Description of the Related Art]

In recent years, there is an increasingly growing demand for an improvement in areal recording density of a magnetic recording medium with an increase in capacity of a magnetic recording disk drive. A reduction in media noise is indispensable for improving the areal recording density. To that end, the grain size of a magnetic layer is required to be made fine for increasing the number of grains per bit. However, microfine magnetic crystal grains become more likely to undergo magnetization reversal due to the influence of thermal fluctuation. Accordingly, the decay of recorded magnetization, that is, the thermomagnetic relaxation phenomenon becomes noticeable. In order to suppress the thermomagnetic relaxation phenomenon, the thermal stability factor ( $Ku \cdot v / kT$ ) is required to be kept at generally 80 to 90 or more, wherein  $Ku$  is the crystal magnetic anisotropy constant,  $v$  is the volume of a magnetic crystal grain,  $k$  is the Boltzmann constant, and  $T$  is the absolute temperature. When the magnetic crystal grain has been made fine, the grain volume  $v$  is reduced. Accordingly,  $Ku$  is required to be raised for keeping  $Ku \cdot v / kT$  at not less than the

aforesaid value. If Ku is improved, the anisotropy field (Hk) is also increased. However, if the Hk exceeds the recording magnetic field from a magnetic head, the overwrite characteristic is largely deteriorated. For this reason, the Hk of the medium is required to be set so as not to exceed the recording magnetic field from the head. This requirement results in the upper limit on the Ku value.

5 [0003]

10 As a technology for ensuring compatibility between the suppression of thermomagnetic relaxation and a reduction in noise, an anti-ferromagnetically coupled medium has been proposed in recent years (Appl. Phys. Lett., vol. 77, pp. 2581-2583, October (2000),  
15 and Appl. Phys. Lett., vol. 77, pp. 3806-3808, December (2000)). This medium is so configured that a magnetic layer portion has a double-layered structure in which respective magnetic layers are anti-ferromagnetically coupled via a Ru intermediate layer therebetween. In  
20 the anti-ferromagnetically coupled medium, the magnetization of a magnetic layer (lower magnetic layer) on the substrate side and the magnetization of another magnetic layer (upper magnetic layer) on the protective layer side are oriented in antiparallel to  
25 each other in the residual magnetization state. For this reason, when the product ( $Br \cdot t$ ) of the residual magnetic flux density (Br) and the magnetic layer thickness (t) is made equal to that of the medium using

a magnetic layer of a single-layered structure, it is possible to increase the thickness of the upper magnetic layer which is a recording layer. Thus, it is possible to raise the thermal stability factor ( $K_u \cdot v/kT$ ) of the magnetic layer.

5

[0004]

However, the foregoing technology falls short of specifically providing a longitudinal magnetic recording medium which has a low noise and a high coercivity, and is also sufficiently stable against thermal fluctuation.

10

[0005]

[Problems to be Solved by the Invention]

15

It is an object of the present invention to provide a longitudinal magnetic recording medium which has a low noise and a high coercivity, and is also sufficiently stable against thermal fluctuation. In addition, it is another object to provide a high reliability magnetic storage apparatus having an areal recording density of 50 megabits per square millimeter or more by combining the longitudinal magnetic recording medium with a high sensitivity magnetic head, and optimizing the read / write conditions.

20

[0006]

25

[Means for Solving the Problems]

In order to achieve the foregoing objects, in accordance with the present invention, the longitudinal magnetic recording medium has been so configured that a

magnetic layer is formed on a non-magnetic substrate via a plurality of underlayers, wherein the magnetic layer is made up of a lower magnetic layer containing at least one of Ru or Re in an amount of not less than 5 3 at% to not more than 30 at%, and Cr in an amount of not less than 0 at% to not more than 18 at%, and further containing at least one of B or C in an amount of not less than 0 at% to not more than 20 at%, and the balance being made up of Co, and an upper magnetic 10 layer containing Co as a main component disposed thereon via a non-magnetic intermediate layer.

[0007]

Further, the plurality of the underlayers has been so configured as to include a non-magnetic and 15 amorphous structured first underlayer containing Co or Ni as a main component, and a body-centered cubic structured second underlayer containing Cr.

[0008]

Further, a B2 structured alloy material may also 20 be used for the first underlayer.

[0009]

Still further, at least one layer of the plurality of the underlayers has been so configured as to be made of a non-magnetic and hexagonal close-packed 25 structured alloy material containing Co.

[0010]

Furthermore, it is also possible that the Co-containing alloy underlayer is formed as a third

underlayer between the lower magnetic layer and the second underlayer.

[0011]

Further, the underlayer made of a non-magnetic and hexagonal close-packed structured alloy material containing Co has been so configured as to be made of a Co-Ru alloy containing Ru in an amount of not less than 35 at% to not more than 60 at%.

[0012]

Still further, at least one layer of the plurality of the underlayers has been so configured as to be made of a Cr-containing body-centered cubic structured alloy material, wherein the Cr alloy contains B in an amount of not less than 2 at% to not more than 15 at%.

[0013]

Furthermore, in a magnetic storage apparatus having: a magnetic recording medium; a driver for driving it in the recording direction; a composite head having an inductive magnetic head for recording and a spin-valve type magnetic head for reading in combination; means for causing the head to perform relative movement with respect to the medium; and a read / write signal processing means with respect to the head, the magnetic recording medium has been allowed to be configured with the longitudinal magnetic recording medium.

[0014]

[Preferred Embodiments of the Invention]

First, a brief description will be given to the embodiments of the present invention.

In an anti-ferromagnetically coupled medium which  
5 is an example of a magnetic recording medium of the present invention, the product ( $Br \cdot t$ ) of the residual magnetic flux density ( $Br$ ) and the magnetic layer thickness ( $t$ ) is generally the difference between the  $Br \cdot t$  of an upper magnetic layer and the  $Br \cdot t$  of a lower  
10 magnetic layer. For this reason, when the  $Br \cdot t$  of the anti-ferromagnetically coupled medium is equally matched with the  $Br \cdot t$  of a single magnetic layer medium using the same magnetic alloy as that of the upper magnetic layer, the  $Br \cdot t$  of the upper magnetic layer  
15 may be set larger by the  $Br \cdot t$  of the lower magnetic layer. The  $Br \cdot t$  of the upper magnetic layer can be increased by mainly increasing the saturation magnetic flux density ( $B_s$ ) or the thickness of the magnetic layer. In the former case, it is possible to increase  
20 the crystal magnetic anisotropy constant ( $K_u$ ) if the anisotropy field ( $H_k$ ) is not reduced. In the latter case, it is possible to increase the volume of the crystal grain ( $v$ ). In consequence, it becomes possible to increase the thermal stability factor ( $K_u \cdot v / kT$ ) ( $k$ :  
25 Boltzmann constant, and  $T$ : the absolute temperature) of the upper magnetic layer. In the anti-ferromagnetically coupled medium, the upper magnetic layer serves as a recording layer. Therefore, by

improving the thermal stability of the magnetic layer, it is possible to suppress the thermomagnetic relaxation phenomenon.

[0015]

5        Accordingly, by setting the  $B_{r,t}$  of the lower magnetic layer at a large value, it is also possible to set the  $B_{r,t}$  of the upper magnetic layer at a large value. As a result, it is possible to more improve the thermal stability. However, in the anti-  
10      ferromagnetically coupled medium, the magnetization of the lower magnetic layer must be oriented in antiparallel to the magnetization of the upper magnetic layer in the residual magnetization state. To that end, the coercivity ( $H_{c2}$ ) of the lower magnetic layer is  
15      required to be made smaller than the coupled magnetic field ( $H_e \times 2$ ) applied on the lower magnetic layer. The  $H_e \times 2$  can be generally described as  $J/(B_{r,t}^2)$  by using the exchange coupling constant ( $J$ ) between the upper magnetic layer and the lower magnetic layer, and the  
20       $B_{r,t}$  ( $B_{r,t}^2$ ) of the lower magnetic layer. For this reason, the  $B_{r,t}^2$  is required to be not more than the  $J/H_{c2}$  for satisfying the foregoing conditions.  
Therefore, in order to increase the  $B_{r,t}^2$  as large as possible, it suffices that the  $J$  is increased, or that  
25      the  $H_{c2}$  is decreased.

[0016]

In order to decrease the  $H_{c2}$ , it is effective to use a material having a small anisotropy field ( $H_k$ ) for

the lower magnetic layer. The general materials currently used for the magnetic layer are hcp structured alloys each containing Co as a main component, and Cr, Pt, or the like, such as Co-Cr-Pt-B and Co-Cr-Pt-Ta alloys. The  $H_k$  of each of these Co alloys mainly depends upon the Pt content, so that it is possible to reduce the  $H_k$  by reducing the Pt content.

[0017]

However, the atomic radius of Pt is larger as compared with that of Co by about 11 %. Therefore, when the Pt content of the lower magnetic layer is reduced, the lattice constant of the magnetic layer is also largely reduced at the same time. Since the upper magnetic layer contains Pt in an amount of 10 to 18 at% as described later, an extreme reduction in the Pt content of the lower magnetic layer results in a significant increase in degree of the lattice misfit between both the magnetic layers. As a result, the epitaxial growth of the upper magnetic layer is inhibited, thereby entailing the problem that the in-plane magnetic anisotropy is largely reduced. In order to prevent this problem, the material having a low  $H_k$ , but having a lattice constant which has not been largely reduced as compared with that of the upper magnetic layer is preferably used for the lower magnetic layer. The present inventors have conducted a study on various materials for the lower magnetic layer. As a result, they have found that the alloy containing

Co as a main component, and containing Ru or Re in place of Pt is most desirable. Although the atomic radius of each of Ru and Re is smaller than that of Pt, it is 68 % larger relative to that of Co.

5 [0018]

Further, even if each of these elements is alloyed with Co, the H<sub>k</sub> is not increased. Therefore, the Co-Ru alloy or the Co-Re alloy can ensure the compatibility between a high lattice constant and a low H<sub>k</sub>. As a result of the study, it has been indicated that the lower magnetic layer may contain Ru or Re in an amount of generally 3 at% or more in order not to inhibit the good epitaxial growth of the upper magnetic layer. However, when each of these elements is added in a large amount, the amount of magnetization of the lower magnetic layer is remarkably reduced. Therefore, the content is desirably 30 at% or less.

15 [0019]

Further, Cr may also be added in an amount of 18 % or less in order to adjust the amount of magnetization. Since Cr has almost the same atomic radius as that of Co, it is capable of adjusting only the amount of magnetization without changing the lattice constant. However, if the amount of Cr added exceeds 18 %, the amount of magnetization is remarkably reduced. In consequence, the effect of canceling the Br·t of the upper magnetic layer is undesirably reduced.

25 [0020]

Further, since the grain size of the upper magnetic layer highly depends upon the grain size of the lower magnetic layer, it is possible to make fine the grain size of the upper magnetic layer by making 5 fine the grain side of the lower magnetic layer. This case is preferable because the media noise can be reduced. In order to make fine the grain size of the lower magnetic layer, the magnetic layer desirably contains B or C in an amount of not less than 0 at% to 10 not more than 20 at%. If the addition amount exceeds 20 at%, the crystalline structure of the lower magnetic layer undesirably undergoes remarkable deterioration. The thickness of the lower magnetic layer is desirably set at 1 nm or more. If it is less than 1 nm, the Br·t 15 of the lower magnetic layer is too small. Accordingly, the Br·t of the upper magnetic layer cannot be set large enough for withstanding the thermal fluctuation.

[0021]

Whereas, in general, when the lower magnetic 20 layer is increased in thickness, the coercivity of the magnetic layer increases. For this reason, if the thickness exceeds a given value, the coercivity of the lower magnetic layer becomes larger than that of the coupled magnetic field applied on the magnetic layer. 25 As a result, the magnetizations of the upper magnetic layer and the lower magnetic layer are not oriented in antiparallel to each other in the residual magnetization state. Consequently, the thickness at

this stage becomes the upper limit of the thickness of the lower magnetic layer. The lower magnetic layer of the present invention has an extremely low  $H_k$ , and hence it also has a low coercivity. Accordingly, even  
5 if it is increased in thickness to about 12 nm, it is possible to cause the magnetizations of the upper magnetic layer and the lower magnetic layer to be oriented in antiparallel to each other in the residual magnetization state. The correlation between the  
10 thickness of the lower magnetic layer and the electromagnetic transfer characteristic varies according to the material of the upper magnetic layer and the underlayer configuration. Therefore, it is desirable that the thickness of the lower magnetic  
15 layer is optimized within a range of 1 nm to 12 nm according to the media configuration.

[0022]

For the upper magnetic layer, it is desirable to use a hcp structured alloy containing Co as a main component, and containing Cr, Pt, B, or the like, such  
20 as CoCrPtB, CoCrPtTa, CoCrPtBCu, or CoCrPtBTa alloy. In order to sufficiently reduce the exchange interaction between magnetic grains, the Cr concentration of the upper magnetic layer is desirably  
25 14 at% or more. However, if the Cr concentration is increased, the crystal magnetic anisotropy constant ( $K_u$ ) is reduced, resulting in a decrease in thermal stability factor ( $K_u \cdot v / kT$ ). Therefore, the Cr content

is desirably 22 at% or less.

[0023]

Further, in order to ensure the compatibility between a high coercivity and a good overwrite characteristic, Pt is desirably contained therein in an amount of not less than 10 at% to not more than 18 at%. Still further, if B is added in an amount of 3 at% or more, the magnetic crystal grains are made fine, and at the same time, the grain boundary segregation of the Cr atoms is promoted. Accordingly, it is possible to largely reduce the media noise. However, since the addition of a large amount of B deteriorates the crystalline structure of the magnetic layer, the addition amount is desirably 18 at% or less. The media noise can also be reduced by adding Ta, Cu, Mo, Zr, W, Ti, SiO<sub>2</sub>, TiO<sub>2</sub>, ZrO<sub>2</sub>, Al<sub>2</sub>O<sub>3</sub>, or the like to the upper magnetic layer. The addition of each of the aforesaid elements or compounds disturbs the hcp structure of the magnetic layer. Therefore, the addition amount is preferably set at 10 at% or less, or 6 mol% or less.

[0024]

As the intermediate layer formed between the lower magnetic layer and the upper magnetic layer, a 0.2 nm - 0.8 nm-thick Ru layer is desirably used. If the Ru layer thickness departs from the aforesaid range, the anti-ferromagnetic coupling between the lower magnetic layer and the upper magnetic layer undesirably decays. As the materials for the intermediate layer,

any materials other than Ru present no problem so long as they are capable of introducing the anti-ferromagnetic coupling between the lower magnetic layer and the upper magnetic layer.

5 [0025]

As the layer configuration of the underlayer, for example, there may be adopted the multi-layered configuration in which a bcc structured second underlayer containing Cr is stacked on a first 10 underlayer made of a non-magnetic and amorphous alloy containing Co, Ni, or the like as a main component. For the first underlayer, for example, there may be desirably used a Co-Crx1-Zry1 ( $x_1$ : 30 to 60 at%, and 15  $y_1$ : 3 to 30 at%), Ni-Crx2-Zry2 ( $x_2$ : 0 to 50 at%, and  $y_2$ : 3 to 60 at%), or Ni-Tax3-Zry3 ( $x_3$ : 3 to 60 at%, and  $y_3$ : 3 to 60 at%), Ni-Tax4 ( $x_4$ : 5 to 60 at%) alloy, or the like. In this case, the grain size of the second underlayer is made fine, and at the same time, it is possible to cause the underlayer to exhibit such an 20 orientation that the (100) plane is generally parallel to the substrate surface (hereinafter, referred to as (100) orientation).

[0026]

Therefore, the lower magnetic layer formed on the 25 second underlayer exhibits such an orientation that the (11.0) plane is generally parallel to the substrate surface (hereinafter, referred to as (11.0) orientation) by epitaxial growth. The upper magnetic

layer also exhibits the (11.0) orientation via the intermediate layer. Accordingly, the grain size of the upper magnetic layer is made fine down to 11 nm or less, suitable for noise reduction, and at the same time, the  
5 c-axis in-plane component is improved. In consequence, it is possible to obtain a medium having a low noise and a strong in-plane magnetic anisotropy. The first underlayer is desirably non-magnetic. However, even if it has a slight magnetization, there is no problem from  
10 the practical viewpoint so long as the saturation magnetic flux density is 0.15 T or less.

[0027]

Further, the first underlayer is not required to have an accurate amorphous structure so long as it does  
15 not exhibit a distinct diffraction peak other than a halo pattern in the X-ray diffraction spectrum, or the mean grain size obtained from the lattice image photographed by a high resolution electron microscope is 5 nm or less. Even the materials for the first  
20 underlayer other than those described above have no particular restriction so long as they are the materials capable of causing the second Cr alloy underlayer to exhibit the (100) orientation, such as MgO, NiP, or Ta. Whereas, when a NiP-plated Al-Mg  
25 alloy is used for a substrate, the Cr alloy layer directly formed on the substrate is (100) oriented, so that particularly, the first underlayer is not required to be formed.

[0028]

For the second underlayer, there may be used bcc structured Cr, Cr-Ti alloy, Cr-Mo alloy, Cr-V alloy, Cr-W alloy, Cr-Mn alloy or the like. The Cr alloy is  
5 preferred since the lattice matching with the magnetic layer is improved because of its larger lattice constant as compared with that of pure Cr. Further, B may also be added thereto in order to make finer the grain size of the second underlayer. In this case, the  
10 grain size of the magnetic layer is also made finer, so that it is possible to further reduce the media noise. However, the addition of B deteriorates the crystalline structure of the underlayer simultaneously with making finer the grain size of the underlayer. Therefore, B  
15 is desirably added in an amount of 15 at% or less. Especially when the amount of B added exceeds 5 at%, for example, the second underlayer may also be configured in double layered structure by forming a Cr layer not containing B, and then forming a CrTiB layer  
20 thereon, or the like. As a result, it is possible to implement the underlayer which has ensured the compatibility between the microfine grain size and the strong (100) orientation.

[0029]

25 The lower magnetic layer may be formed directly on the second underlayer. Alternatively, a Co-containing hcp structured non-magnetic alloy layer may also be provided between the underlayer and the

magnetic layer as a third underlayer. In this case,  
the lower magnetic layer is epitaxially grown on the  
underlayer having the same crystal structure (hcp  
structure). Therefore, it undergoes good crystal  
5 growth from the initial growth state. For this reason,  
the crystalline structure of the upper magnetic layer  
and the in-plane orientation of the c-axis are also  
improved, so that it is possible to obtain a medium  
having a high coercivity. The material for the third  
10 underlayer has no particular restriction so long as it  
is an alloy material having a hcp structure and a  
saturation magnetic flux density of 0.15 T or less,  
such as a Co-Cr alloy or a Co-Cr-Pt alloy. However,  
when a Co-Ru alloy containing Ru in an amount of not  
15 less than 35 at% to not more than 60 at% is used,  
particularly desirably, the lattice matching is  
improved, so that it is possible to reduce the media  
noise.

[0030]

20 The aforesaid underlayer configuration causes all  
the magnetic layers to have the (11.0) orientation.  
However, the orientation of the magnetic layer may be  
the (10.0) orientation with the c-axis of the magnetic  
alloy facing in the in-plane direction as with the  
25 (11.0) orientation. In order for the magnetic layer to  
have the (10.0) orientation, a B2 structured alloy such  
as a Ni-50at% Al alloy may be desirably used for the  
first underlayer. In this case, the second underlayer

mainly exhibits the (211) orientation, and hence the third underlayer and the magnetic layer have the (10.0) orientation due to epitaxial growth. Even in the case in which the magnetic layer is (10.0)-oriented, the  
5 same effect as that for the (11.0) orientation can be obtained by using an alloy material containing Co as a main component, and containing Ru, Cr, B, or C of the present invention for the lower magnetic layer.

[0031]

10 By forming a nitrogen-doped carbon layer with a thickness of 3 nm to 7 nm as a protective layer, and further providing a lubricant layer of adsorptive perfluoroalkyl-polyether, or the like with a thickness of 1 nm to 4 nm, it is possible to obtain a high  
15 reliability magnetic recording medium capable of performing high density recording. Further, if a hydrogen-doped carbon layer, or a layer made of a compound such as silicon carbide, tungsten carbide, (W-Mo)-C, or (Zr-Nb)-N, or a mixed layer of any of the  
20 compounds and carbon is used as the protective layer, preferably, the durability against sliding and the corrosion resistance can be improved.

[0032]

As the substrate, there may be used, other than  
25 chemically strengthened aluminosilicate, ceramics made of soda-lime glass, silicon, borosilicate glass, or the like, glass-glazed ceramics, Ni-P non-electrolysis plated Al-Mg alloy substrate, or Ni-P sputtered glass

substrate, or rigid substrate made of Ni-P non-electrolysis plated glass, etc., or the like.

[0033]

As for the magnetic characteristics of the anti-  
5 ferromagnetically coupled medium of the present  
invention, it is desirable that the coercivity is not  
less than 240 kA/m (3,024 Oe) to not more than 400 kA/m  
(5,040 Oe), and that the residual magnetization ( $Br \cdot t$ )  
is not less than 2.0 Tnm (20G·μm) to not more than 6.0  
10 Tnm (60G·μm). Herein, the residual magnetization is  
generally the value obtained by subtracting the  $Br \cdot t$  of  
the lower magnetic layer from the  $Br \cdot t$  of the upper  
magnetic layer, and it is the value corresponding to O·  
Q of FIG. 1. If the coercivity is less than 240 kA/m,  
15 the recording resolution is reduced. Whereas, if it  
exceeds 400 kA/m, the overwrite characteristic is  
deteriorated. Thus, both the cases are undesirable.

[0034]

Further, if the residual magnetization is less  
20 than 2.0 Tnm, the read output is reduced. Whereas, if  
it exceeds 6.0 Tnm, high resolution cannot be obtained.  
Thus, both the cases are undesirable.

[0035]

The graph of FIG. 1 shows one example of the  
25 hysteresis loop of the anti-ferromagnetically coupled  
medium of the present invention. The magnetization of  
the lower magnetic layer is required to be oriented in  
antiparallel to the magnetization of the upper magnetic

layer in the residual magnetization state. For this reason, the magnetic field at which the magnetization reversal of the lower magnetic layer is completed (point P in the figure) must be a positive value.

5 Further, in order to sufficiently suppress the thermomagnetic relaxation phenomenon, the thermal stability factor ( $Ku \cdot v / kT$ ) is desirably 80 to not less than 90. The thermal stability factor can be determined by fitting the time dependence of the

10 remanence coercivity in the Sharrock's equation as described in, J. Magn. Magn. Mater. 127, p. 233 (1993), for example. From the study by the present inventors, it has been concluded as follows: if the  $Ku \cdot v / kT$  at room temperature determined in this manner is 80 to not

15 less than 90, the decay in read output at 5 years later is estimated to be 10 % or less, thus presenting no problem in terms of reliability.

[0036]

Further, in a magnetic storage apparatus having a

20 magnetic recording medium, a driver for driving it in the recording direction, a magnetic head made up of a write element and a read element, means for causing the magnetic head to perform relative movement with respect to the magnetic recording medium, and a read / write

25 signal processing means for performing the signal input to the magnetic head and the output signal read-back from the magnetic head, by using any of the aforesaid media for the magnetic recording medium, it is possible

to provide a high reliability magnetic storage apparatus having an areal recording density of 50 Mbit/mm<sup>2</sup> or more.

[0037]

5       Namely, the read element of the magnetic head is configured with a spin-valve type sensor including a plurality of conductive magnetic layers of which mutual magnetization directions are relatively changed by the external magnetic field to generate a large resistance  
10      change, and conductive non-magnetic layers disposed each between the conductive magnetic layers. The sensor element is desirably formed between the two shield layers made of a soft magnetic material separated by a distance of 0.10 μm or less from one  
15      another. This is attributable to the following fact. Namely, if the distance between shields is 0.10 μm or more, the resolution is reduced, so that the phase jitter of a signal increases. By implementing the aforesaid configuration of the storage apparatus, it is  
20      possible to further raise the signal intensity. As a result, it becomes possible to implement a high reliability magnetic storage apparatus having a recording density of 50 Mbit/mm<sup>2</sup> or more.

[0038]

25      Below, the detailed examples of the present invention will be further described in details by reference to drawings.

<Example 1>

FIG. 2 is a cross sectional view of the configuration of one embodiment of a magnetic recording medium of the present invention. As a substrate 11, a 0.635 mm-thick and 2.5-dia type aluminosilicate glass substrate of which surface had been chemically strengthened was used. This substrate was subjected to alkali cleaning. Subsequently, the following multi-layered film was formed with a tact of 9 sec by means of a sheet-fed type sputtering apparatus (NDP250B) manufactured by Intervac Co. The chamber configuration or the station configuration of this sputtering apparatus is shown in FIG. 3. First, in a charging chamber 20, the substrate 11 was kept under vacuum, and in a first underlayer forming chamber 21, first underlayers 12 each made of a 30 nm-thick Ni-37.5at% Ta alloy were formed on both the sides of the substrate 11. Thereafter, in a heating chamber 22, heating was conducted in a mixed gas atmosphere of an Ar gas and oxygen by a lamp heater so that the temperature of the substrate is about 240 °C. In a second underlayer forming chamber 23, second underlayers 13 each made of a 10 nm-thick Cr-20at% Ti alloy were formed respectively thereon.

[0039]

Further, subsequently, in a third underlayer forming chamber 24, third underlayers 14 each made of a 3 nm-thick Co-40at% Ru alloy were formed respectively thereon. Then, in a lower magnetic layer forming

chamber 25, lower magnetic layers 15 each made of a 2  
to 10 nm-thick Co-24at% Ru-8at% B alloy were formed  
respectively thereon. In an intermediate layer forming  
chamber 26, 0.4 nm-thick Ru intermediate layers 16 were  
5 formed respectively thereon. Then, in an upper  
magnetic layer forming chamber 27, 18 nm to 21 nm-thick  
upper magnetic layers 17 each made of Co-18at% Cr-14at%  
Pt-8at% B alloy were formed respectively thereon. In  
two protective layer forming chambers 28 and 28',  
10 protective layers 18 each having a total thickness of 4  
nm were formed respectively thereon. Table 1 shows the  
combinations of the thickness of the lower magnetic  
layer and the thickness of the upper magnetic layer.  
Subsequently, the substrate was taken out from the  
15 sputtering apparatus. Then, a lubricant containing  
perfluoroalkyl-polyether as a main component was  
applied on the protective layers to form 1.8 nm-thick  
lubricant layers 19.

[0040]

20 For forming the first underlayers 12, the second  
underlayers 13, the third underlayers 14, the lower  
magnetic layers 15, the intermediate layers 16, and the  
upper magnetic layers 17, Ar was used as a discharge  
gas in all the cases. The gas pressure was set at 5.3  
25 Pa (40 mTorr) only for depositing the lower magnetic  
layers, and at 0.93 Pa (7 mTorr) for depositing other  
layers. Further, for forming the protective layers 18  
made of carbon, Ar containing nitrogen was used as the

discharge gas, and the pressure thereof was set at 1.33 Pa (10 mTorr).

[0041]

The magnetic recording medium formed in this manner was cut, and the laminated thin film portion was reduced in thickness in a mortar form vertically along the direction perpendicular to the layer surface by an ion thinning method. Thus, the microfine structure of the first underlayer was observed by means of a transmission electron microscope with an acceleration voltage of 200 kV. As a result, the crystal grain size was found to be 5 nm or less. Further, upon photographing the selected-area electron diffraction image, a halo was observed. Accordingly, it has been confirmed that the structure is substantially an amorphous structure.

[0042]

The magnetic characteristics of the magnetic disk medium obtained were evaluated by a coercivity measuring apparatus utilizing the Kerr effect and a vibrating sample magnetometer (VSM). From the magnetic disk, 8 mm square samples were cut to be used as test samples for VSM. The measurement of the magnetic characteristics by VSM was carried out at room temperature by applying a magnetic field of up to 800 kA/m at maximum in the circumferential direction of the medium. Table 2 shows the magnetic characteristics corresponding to their respective sample Nos. shown in

Table 1. The coercivities  $H_c$  determined by using the Kerr effect were less than 300 kA/m for the sample Nos. 101, 102, and 106. For the samples having coercivities in excess of 300 kA/m, the magnetic characteristics were evaluated by VSM. The thermal stability factor ( $K_u \cdot v / kT$ ) was determined by approximating the time dependence of the remanence coercivity at 7.5 sec to 240 sec at room temperature to the Sharrock's equation. Incidentally, the measurements of the remanence coercivity were carried out for 6 points at 7.5, 15, 30, 60, 120, and 240 sec later.

[0043]

Table 1

Sample No.	Lower magnetic layer	Intermediate layer	Upper magnetic layer
	Co-24at% Ru-8at% B (nm)	Ru (nm)	Co-18at% Cr-14at% Pt-8at% B (nm)
101	10.0	0.4	18.0
102	8.0	↑	18.0
103	6.0	↑	18.0
104	4.0	↑	18.0
105	2.0	↑	18.0
106	10.0	↑	19.5
107	8.0	↑	19.5
108	6.0	↑	19.5
109	4.0	↑	19.5
110	2.0	↑	19.5
111	10.0	↑	21.0
112	8.0	↑	21.0
113	6.0	↑	21.0
114	4.0	↑	21.0
115	2.0	↑	21.0

Table 2

Sample No.	Kerr	VSM			
	Hc (kA/m)	Hc (kA/m)	S*	Br·t (T·nm)	Ku·v/kT
101	241	-	-	-	-
102	264	-	-	-	-
103	328	249	0.83	2.7	79
104	328	276	0.70	3.9	84
105	334	295	0.71	4.8	83
106	260	-	-	-	-
107	320	237	0.68	2.1	81
108	331	249	0.59	3.2	84
109	333	289	0.73	4.3	87
110	339	306	0.74	5.5	90
111	319	187	0.50	1.9	78
112	333	240	0.72	2.4	84
113	334	270	0.72	3.5	85
114	334	290	0.70	5.2	93
115	339	304	0.72	5.9	93

Not depending upon the thickness of the upper magnetic layer, if the thickness of the lower magnetic layer was increased, the coercivity, the product (Br·t) of the residual magnetic flux density Br and the thickness t of the magnetic layer, the thermal stability factor (Ku·v/kT), and the like were reduced. For example, in the medium in which the thickness of the upper magnetic layer had been set at 21 nm, when the thickness of the lower magnetic layer was increased up to 2 nm to 10 nm, the coercivity decreased to 304 kA/m to 187 kA/m, the Br·t decreased to 5.9 Tnm to 1.9 Tnm, and the Ku·v/kT decreased to 93 to 78, respectively. FIG. 4 shows the enlarged view of a portion at a magnetic field of around zero of each

hysteresis loop of the sample Nos. 111 to 114. For any of the media, steps are observed in the hysteresis loop in the area in which the magnetic field is positive (upper right quadrant region).

5 [0044]

This indicates as follows. When the magnetic field has been set at zero, the magnetization reversal of the lower magnetic layer is completed. Thus, in the residual magnetization state, the magnetization of the 10 lower magnetic layer is oriented in antiparallel to the magnetization of the upper magnetic layer. In consequence, it has been shown that, in each of the media of this example, even if the thickness of the lower magnetic layer is increased to 10 nm, the 15 magnetizations of the upper magnetic layer and the lower magnetic layer are oriented in antiparallel to each other in the residual magnetization state.

[0045]

The evaluation of the electromagnetic transfer characteristics was carried out by using a composite head made up of a GMR head having a shield gap length of 0.10  $\mu\text{m}$  and a track width for read (Twr) of 0.33  $\mu\text{m}$ , and a writing head having a gap length of 0.14  $\mu\text{m}$ . The linear recording density which was 1/6 the maximum 25 linear recording density (HF) was set for 1F of the overwrite characteristic, wherein the maximum linear recording density (HF) was 24.8 kFC/mm (630 kFCI). The electromagnetic transfer characteristics corresponding

to the sample Nos. shown in Table 1 are shown in Table  
3. If the lower magnetic layer is increased in  
thickness not depending upon the thickness of the upper  
magnetic layer, the output half-width (PW50) of the  
solitary reproduction wave decreased, and the output  
resolution (ReMF) at the linear recording density (MF)  
which was half the maximum linear recording density was  
improved. Further, at this step, the overwrite  
characteristic (OW) was also improved.

10 [0046]

Table 3

Sample No.	So ( $\mu$ Vpp)	PW50 (nm)	OW (dB)	ReMF (%)	Nd/So ( $\mu$ Vrms/ $\mu$ Vpp)	Media S/N (dB)
103	954	116	42	53.3	0.0417	22.1
104	1250	120	37	49.0	0.0384	22.1
105	1486	123	36	48.8	0.0394	21.9
108	1055	117	41	51.2	0.0391	22.3
109	1375	123	36	47.6	0.0384	21.9
110	1592	125	36	47.9	0.0391	21.8
113	1163	118	40	50.9	0.0384	22.4
114	1440	124	36	47.3	0.0398	21.5
115	1640	127	35	47.9	0.0412	21.3

On the other hand, the normalized media noise  
(Nd/So) obtained by normalizing the media noise (Nd)  
when recording was performed at HF with a solitary  
reproduction wave output (So) exhibited different lower  
magnetic layer thickness dependencies according to the  
thickness of the upper magnetic layer. In the case  
where the lower magnetic layer thickness was increased  
to 2 nm to 6 nm when the thickness of the upper  
magnetic layer was 18.0 mm, the Nd/So increased about  
15  
20

6 %. In contrast, it decreased about 7 % when the thickness of the upper magnetic layer was 21.0 nm. Further, the media S/N showed the highest value when the upper magnetic layer thickness was set at 21 nm,  
5 and the lower magnetic layer thickness was increased to 6 nm. Herein, the media S/N is the value defined as media S/N = 20 log (SMF/Nd) by using the read output at MF (SMF) and Nd.

[0047]

10 When a Co-32at% Cr-6at% Zr, Co-36at% Cr-8at% Ta, Co-40at% V-8at% B, or Co-50at% V-12at% Si alloy was used in place of the Ni-37.5at% Ta alloy for the first underlayer, in combination with the magnetic layer of the sample No. 113, a particularly low normalized noise  
15 was shown. Further, for the medium using a Ni-40at% Cr-8at% Zr, or Ni-55at% V-15at% Si alloy for the first underlayer, a particularly high coercivity of 360 kA/m or more was obtained.

[0048]

20 <Example 2>  
Media each having the same layer configuration as that in Example 1, except that a Co-24at% Ru-10at% B alloy was used as the lower magnetic layer were formed through the same deposition process as that in Example  
25 1. Table 4 shows the combinations of the thickness of the lower magnetic layer and the thickness of the upper magnetic layer, and Table 5 shows the magnetic characteristics thereof. From the comparison between

the magnetic characteristics shown in Tables 2 and 5, it has been shown that, when the same thickness is adopted for each upper magnetic layer, use of the Co-24at% Ru-10at% B alloy provides larger  $H_c$ ,  $B_{r.t}$ , and  
5  $Ku \cdot v/kT$  than with the use of Co-24at% Ru-8at% B alloy for the lower magnetic layer.

[0049]

The electromagnetic transfer characteristics of disks having their respective magnetic characteristics of Table 5 were evaluated by using the magnetic head used for the disk evaluation in Example 1. As a result, as shown in Table 6, it has been shown as follows.  
10 Namely, when the Co-24at% Ru-10at% B has been used for the lower magnetic layer, if the thickness of the lower magnetic layer is increased to 2 nm to 6 nm, not depending upon the thickness of the upper magnetic layer, (1) PW50 shortens; (2) the overwrite characteristic and the media S/N are improved; and (3)  
15 the Nd/So decreases. Especially when the thickness of the upper magnetic layer has been set at 21 nm, the decrease in Nd/So is noticeable.  
20

[0050]

Table 4

Sample No.	Lower magnetic layer	Intermediate layer	Upper magnetic layer
	Co-24at% Ru-10at% B (nm)	Ru (nm)	Co-18at% Cr-14at% Pt-8at% B (nm)
201	10.0	0.4	18.0
202	8.0	↑	18.0
203	6.0	↑	18.0
204	4.0	↑	18.0
205	2.0	↑	18.0
206	10.0	↑	19.5
207	8.0	↑	19.5
208	6.0	↑	19.5
209	4.0	↑	19.5
210	2.0	↑	19.5
211	10.0	↑	21.0
212	8.0	↑	21.0
213	6.0	↑	21.0
214	4.0	↑	21.0
215	2.0	↑	21.0

Table 5

Sample No.	Kerr	VSM			
	Hc (kA/m)	Hc (kA/m)	S*	Br·t (T·nm)	Ku·v/kT
201	227	-	-	-	-
202	260	-	-	-	-
203	318	252	0.77	3.2	81
204	324	268	0.77	4.3	84
205	336	308	0.75	5.2	90
206	311	-	-	-	-
207	316	237	0.69	2.8	81
208	321	253	0.75	3.8	84
209	329	283	0.73	5.0	89
210	341	309	0.74	6.1	93
211	313	206	0.54	2.3	82
212	321	254	0.70	3.4	86
213	324	277	0.73	4.4	93
214	328	287	0.73	5.7	94
215	342	319	0.73	6.8	99

Table 6

Sample No.	So ( $\mu$ Vpp)	PW50 (nm)	OW (dB)	ReMF (%)	Nd/So ( $\mu$ Vrms/ $\mu$ Vpp)	Media S/N (dB)
203	1072	119	41	50.7	0.0369	22.8
204	1346	123	37	47.8	0.0396	21.6
205	1559	125	36	47.9	0.0393	21.7
208	1231	120	39	48.7	0.0351	22.8
209	1507	125	35	47.1	0.0390	21.6
210	1681	126	36	47.6	0.0398	21.6
213	1370	123	38	48.0	0.0347	22.8
214	1608	128	35	46.4	0.0402	21.2
215	1781	129	34	46.8	0.0413	21.1

## &lt;Example 3&gt;

Media each having the same layer configuration as  
 5 that in Example 1 were formed, except for changing (1) the substrate temperature, (2) the thickness of the CrTi underlayer, and (3) the thickness of the Ru intermediate layer. The deposition process was the same as that in Example 1, except that the Ar gas  
 10 pressure during deposition of the lower magnetic layer was set at 0.93 Pa. Tables 7 to 9 show the relationship between the layer configuration of each medium and the sample number, the magnetic characteristics, and the electromagnetic transfer  
 15 characteristics. Incidentally, a head having a Twr = 0.35  $\mu$ m was used for the evaluation of the electromagnetic transfer characteristics. Any of the media showed a high coercivity of 260 kA/m or more, and a low normalized media noise of 0.04  $\mu$ Vrms/ $\mu$ Vpp or less.

[0051]

Table 7

Sample No.	Substrate temperature (°C)	Second underlayer Cr-20at% Ti (nm)	Lower magnetic layer Co-24at% Ru-8at% B (nm)	Intermediate layer Ru (nm)	Upper magnetic layer Co-18at% Cr-14at% Pt-8at% B (nm)
301	210	10	2.0	0.4	18.0
302	240	10	↑	↑	↑
303	270	15	↑	↑	↑
304	↑	5	↑	↑	↑
305	↑	10	↑	0.8	↑
306	↑	↑	↑	0.6	↑
307	↑	↑	↑	0.4	↑
308	↑	↑	↑	0.2	↑
309	300	↑	↑	↑	↑

Table 8

Sample No.	Hc (kA/m)	S*	Br·t (T·nm)	Ku·v/kT
301	264	0.80	5.0	78
302	298	0.72	5.1	88
303	338	0.72	5.2	105
304	295	0.66	5.4	89
305	317	0.63	5.4	101
306	326	0.70	5.4	100
307	331	0.68	5.2	103
309	345	0.69	4.8	118

5

Table 9

Sample No.	So (μVpp)	PW50 (nm)	OW (dB)	ReMF (%)	Nd/So (μVrms/μVpp)	Media S/N (dB)
301	1107	125.7	37	48	0.0400	21.6
302	1132	125.2	36	48	0.0372	22.3
303	1097	125.2	36	49	0.0391	22.0
304	1153	126.6	36	48	0.0356	22.6
305	1154	128.1	35	48	0.0379	22.0
306	1116	126.8	35	48	0.0385	21.9
307	1127	125.4	35	48	0.0384	22.0
309	1059	125.3	35	49	0.0378	22.2

The Hc and the Ku·v/kT tended to increase with an

increase in substrate temperature, but that the media S/N became maximum when the substrate temperature was 240 °C. The Hc and the Ku·v/kT increased also when the CrTi underlayer was increased in thickness. The  
5 Nd/So of the medium (sample No. 304) in which the thickness of the CrTi underlayer had been decreased to 5 nm was minimum, indicating that a decrease in thickness of the CrTi underlayer is effective for noise reduction. On the other hand, the change in  
10 electromagnetic transfer characteristics with the change in thickness of the Ru intermediate layer was small, and the characteristics were generally constant within a range of 0.2 to 0.8 nm. Whereas, for evaluating the magnetic characteristics of the Co-24at%  
15 Ru-8at% B alloy used for the lower magnetic layer, a medium in which the thickness of the magnetic layer had been set at 18 nm and the upper magnetic layer had not been formed was manufactured. The magnetization curve was measured by applying a magnetic field in the in-  
20 plane direction. As a result, the coercivity and the saturation magnetic flux density were 8.8 kA/m and 0.60 T, respectively.

[0052]

<Example 4>

25 Media each having the same layer configuration as that in Example 2 were formed, except for changing (1) the substrate temperature, (2) the thickness of the CrTi underlayer, and (3) the thickness of the Ru

intermediate layer. Tables 10 to 12 show the relationship between the layer configuration of each medium and the sample number, the magnetic characteristics, and the electromagnetic transfer characteristics evaluated by the head used in Example 3, respectively. Any of the media showed a high  $H_c$  of 250 kA/m or more, and a high media S/N of 21.5 dB or more.

5 As with Example 3, both of the  $H_c$  and the  $Ku \cdot v/kT$  increased with an increase in substrate temperature and

10 an increase in thickness of the CrTi underlayer. However, both values of the  $H_c$  and the  $Ku \cdot v/kT$  were slightly smaller as compared with those of the media of Example 3. Further, the medium (sample No. 404) in which the thickness of the CrTi underlayer had been

15 decreased to 5 nm had the lowest noise, and had the maximum media S/N.

[0053]

Table 10

Sample No.	Substrate temperature (°C)	Second underlayer Cr-20at% Ti (nm)	Lower magnetic layer Co-24at% Ru-10at% B (nm)	Intermediate layer Ru (nm)	Upper magnetic layer Co-18at% Cr-14at% Pt-8at% B (nm)
401	210	10	2.0	0.4	18.0
402	240	10	↑	↑	↑
403	270	15	↑	↑	↑
404	↑	5	↑	↑	↑
405	↑	10	↑	0.8	↑
406	↑	↑	↑	0.6	↑
407	↑	↑	↑	0.4	↑
408	↑	↑	↑	0.2	↑
409	300	↑	↑	↑	↑

Table 11

Sample No.	Hc (kA/m)	S*	Br·t (T·nm)	Ku·v/kT
401	254	0.80	5.5	71
402	286	0.68	5.4	84
403	322	0.71	5.3	103
404	281	0.69	5.3	85
405	318	0.69	5.4	100
406	312	0.64	5.4	99
407	314	0.60	5.6	99
409	336	0.68	5.5	115

Table 12

Sample No.	So ( $\mu$ Vpp)	PW50 (nm)	OW (dB)	ReMF (%)	Nd/So ( $\mu$ Vrms/ $\mu$ Vpp)	Media S/N (dB)
401	1197	128	36	48	0.0399	21.5
402	1179	128	35	48	0.0364	22.3
403	1117	128	35	49	0.0387	22.0
404	1181	127	36	47	0.0349	22.5
405	1164	129	35	48	0.0372	22.1
406	1130	128	35	48	0.0376	22.2
407	1151	127	35	48	0.0371	22.2
409	1122	128	35	48	0.0379	22.0

As for the media of this example, there were not  
 5 observed large differences in electromagnetic transfer  
 characteristics as compared with those of the media of  
 Example 3. The coercivity and the saturation magnetic  
 flux density of the Co-24at% Ru-10at% B alloy used for  
 the lower magnetic layer were determined in the same  
 10 manner as in Example 3, and found to be 7.6 kA/m and  
 0.56 T, respectively.

[0054]

<Example 5>

The media in each of which a 25 nm-thick Co-30at%  
 15 Cr-10at% Zr alloy layer was used as the first

underlayer, and a Co-20at% Cr-14at% Pt-6at% B alloy layer was used as the upper magnetic layer were manufactured. The layer configuration and the deposition process are the same as in Example 1. Table 5 13 shows the set values of (1) the substrate temperature, (2) the thickness of the second underlayer, (3) the thickness of the lower magnetic layer, (4) the thickness of the Ru intermediate layer, and (5) the thickness of the upper magnetic layer. Table 14 shows 10 the respective magnetic characteristics corresponding to the media. The  $K_u \cdot v/kT$  increases up to 330 °C with an increase in substrate temperature, but the coercivity tends to be saturated at 300 °C or more. Further, the coercivity squareness  $S^*$  of each medium of 15 this example was smaller as compared with the  $S^*$  of each medium of examples shown in Examples 1 to 4. Table 15 shows the electromagnetic transfer characteristics of respective media evaluated by the head in which  $T_{wr} = 0.33 \mu\text{m}$ . As for each of the media 20 other than the medium of the sample No. 508 in which the thickness of the lower magnetic layer was 6 nm, the  $Nd/So$  was as low as 0.04  $\mu\text{V}_{rms}/\mu\text{V}_{pp}$  or less, and the media S/N was as large as 22.0 dB or more. From the fact that the highest S/N is obtainable when the 25 thickness of the lower magnetic layer is 1 nm, it has been shown that the optimum value of the thickness of the lower magnetic layer also depends upon the composition of the upper magnetic layer.

[0055]

Table 13

Sample No.	Substrate temperature (°C)	Second underlayer Cr-20at% Ti (nm)	Lower magnetic layer Co-24at% Ru-8at% B (nm)	Intermediate layer Ru (nm)	Upper magnetic layer Co-20at% Cr-14at% Pt-6at% B (nm)
501	270	20	2.0	0.4	18.0
502	300	↑	↑	↑	↑
503	330	25	↑	↑	↑
504	↑	15	↑	↑	↑
505	↑	↑	↑	0.6	↑
506	↑	↑	↑	0.4	↑
507	↑	↑	↑	0.2	↑
508	↑	↑	6.0	↑	↑
509	↑	↑	4.0	↑	↑
510	↑	↑	1.0	↑	↑
511	↑	↑	2.0	↑	16.5
512	↑	↑	↑	↑	19.5

Table 14

Sample No.	Hc (kA/m)	S*	Br·t (T·nm)	Ku·v/kT
501	284	0.61	5.2	96
502	306	0.59	5.1	110
503	329	0.61	5.0	128
504	279	0.45	4.8	98
505	302	0.48	4.9	119
506	305	0.54	4.8	120
507	303	0.45	4.8	122
508	202	0.23	2.7	95
509	251	0.46	3.6	108
510	313	0.46	5.2	115
511	295	0.41	4.6	116
512	305	0.48	5.4	122

Table 15

Sample No.	So ( $\mu$ Vpp)	PW50 (nm)	OW (dB)	ReMF (%)	Nd/So ( $\mu$ Vrms/ $\mu$ Vpp)	Media S/N (dB)
501	1184	128	37	48	0.0377	22.1
502	1140	127	37	48	0.0367	22.3
503	1105	128	38	48	0.0381	22.0
504	1071	128	39	47	0.0358	22.4
505	1113	128	38	48	0.0369	22.3
506	1103	127	38	48	0.0366	22.3
507	1108	129	38	47	0.0371	22.1
508	646	111	39	56	0.0595	19.5
509	844	121	42	48	0.0360	22.5
510	1170	128	38	47	0.0368	22.2
511	1043	125	39	49	0.0365	22.5
512	1188	131	37	47	0.0374	22.0

## &lt;Example 6&gt;

The media each having the same layer

5 configuration in Example 5 were manufactured, except that a Co-18at% Cr-14at% Pt-6at% B-2at% Cu alloy was used for the upper magnetic layer. Table 16 shows the set values of (1) the substrate temperature, (2) the thickness of the second underlayer, (3) the thickness 10 of the lower magnetic layer, (4) the thickness of the Ru intermediate layer, and (5) the thickness of the upper magnetic layer. The Co-Cr-Pt-B-Cu alloy used for the upper magnetic layer in this example has a saturation magnetic flux density which is about 20 % higher than that of the Co-Cr-Pt-B alloy used in Example 15. Therefore, the standard thickness of the upper magnetic layer was set at 15.0 nm. The magnetic characteristics of the respective media shown in Table 16 are shown in Table 17. It was possible to obtain

media each having a high coercivity of 240 kA/m or more except for the sample No. 608. Further, from the comparison between the medium of a sample No. 612 and the medium of a sample No. 511 of Example 5, it has  
5 been shown that, when an equal thickness is adopted, use of the Co-Cr-Pt-B-Cu alloy of this example for the upper magnetic layer provides a higher coercivity and a higher  $K_u \cdot v / kT$  than with the use of the Co-Cr-Pt-B alloy of Example 5.

10 [0056]

Table 16

Sample No.	Substrate temperature (°C)	Second underlayer Cr-20at% Ti (nm)	Lower magnetic layer Co-24at% Ru-8at% B (nm)	Intermediate layer Ru (nm)	Upper magnetic layer Co-18at% Cr-14at% Pt-6at% B-2at% Cu (nm)
601	270	20	2.0	0.4	15.0
602	300	↑	↑	↑	↑
603	330	25	↑	↑	↑
604	↑	15	↑	↑	↑
605	↑	↑	↑	0.6	↑
606	↑	↑	↑	0.4	↑
607	↑	↑	↑	0.2	↑
608	↑	↑	6.0	↑	↑
609	↑	↑	4.0	↑	↑
610	↑	↑	1.0	↑	↑
611	↑	↑	2.0	↑	13.5
612	↑	↑	↑	↑	16.5

Table 17

Sample No.	Hc (kA/m)	S*	Br·t (T·nm)	Ku·v/Kt
601	270	0.63	4.8	97
602	287	0.54	4.5	104
603	322	0.42	4.6	121
604	247	0.49	4.4	97
605	287	0.41	4.7	114
606	291	0.39	4.6	113
607	293	0.38	4.8	115
608	183	0.14	2.1	95
609	246	0.39	3.4	108
610	303	0.43	5.0	116
611	277	0.38	4.2	105
612	308	0.48	4.9	125

Table 18 shows the electromagnetic transfer characteristics of each disk. The head used for the evaluation has a write gap length 0.14  $\mu\text{m}$ , a shield gap length of 0.10  $\mu\text{m}$ , and a Twr = 0.33  $\mu\text{m}$ . The head flying height hm (the distance between the surface of the upper magnetic layer and the surface of the main pole) was set at 24 nm, and the circumferential speed was set at 7 m/s. The medium (sample No. 604) in which the thickness of the second underlayer had been decreased to 10 nm, and the medium (sample No. 609) in which the thickness of the lower magnetic layer had been decreased to 4.0 nm showed the lowest Nd/So, and a high media S/N of 22.6 dB or more. Table 19 shows the results when the measurements have been carried out by using another head in which the write gap length and the shield gap length have been the same as before, and the hm has been set at 23 nm. Also in this case,

relatively lower Nd/So values were obtained for the media of the sample Nos. 604 and 609.

[0057]

Table 18

Sample No.	So ( $\mu$ Vpp)	PW50 (nm)	OW (dB)	ReMF (%)	Nd/So ( $\mu$ Vrms/ $\mu$ Vpp)	Media S/N (dB)
601	1711	129	39	50	0.0395	22.1
602	1660	129	39	49	0.0379	22.3
603	1611	129	38	50	0.0382	22.2
604	1576	130	40	48	0.0353	22.6
605	1609	130	39	48	0.0368	22.3
606	1581	130	40	49	0.0369	22.4
607	1621	130	40	48	0.0367	22.3
608	807	114	41	56	0.0699	18.1
609	1180	124	41	49	0.0352	22.8
610	1664	129	40	49	0.0373	22.4
611	1415	127	41	50	0.0371	22.5
612	1677	132	38	47	0.0374	22.0

5

Table 19

Sample No.	So ( $\mu$ Vpp)	PW50 (nm)	OW (dB)	ReMF (%)	Nd/So ( $\mu$ Vrms/ $\mu$ Vpp)	Media S/N (dB)
604	1113	127	39	50	0.0379	22.4
606	1142	126	39	51	0.0388	22.4
608	610	99	40	58	0.0734	18.0
609	850	120	42	51	0.0374	22.7
610	1212	126	39	50	0.0388	22.3
611	1046	124	40	51	0.0385	22.4
612	1236	129	38	50	0.0395	22.0

<Example 7>

The media each having the same layer

10 configuration in Example 1 were manufactured, except that a Ni-20at% Cr-10at% Zr alloy was used for the first underlayer, and a Cr-40 at% MoB alloy was used for the second underlayer, and a 2 to 6 nm-thick Co-16at% Ru, Co-16at% Ru-3at% B, Co-16at% Ru-10at% B, Co-

16at% Ru-20at% B, Co-16at% Ru-23at% B, Co-30at% Ru-8at%  
B, Co-3at% Ru-8at% B, Co-10at% Ru-5at% Cr, Co-3at% Ru-  
18at% Cr-6at% B, Co-14at% Ru-5at% C, or Co-14at% Ru-  
5at% Cr-5at% C alloy was used for the lower magnetic  
5 layer. A 19 nm-thick Co-16at% Cr-12at% Pt-12at% B  
alloy was used for the upper magnetic layer. Whereas,  
as a comparative example, a medium in which a Ru-free  
Co-18at% Cr-9at% Pt-6at% B alloy was used for the lower  
magnetic layer was manufactured. Each magnetization  
10 curve was measured, and, for any of the media, steps  
have been observed in the area in which the magnetic  
field is positive in the magnetization curve. This has  
indicated that the magnetizations of the upper magnetic  
layer and the lower magnetic layer are oriented in  
15 antiparallel to each other in the residual  
magnetization state. Table 20 shows the  
electromagnetic transfer characteristics evaluated by  
using the magnetic head described in Example 1.

[0058]

Table 20

Sample No.	Lower magnetic layer	So ( $\mu$ Vpp)	OW (dB)	Nd/So ( $\mu$ Vrms/ $\mu$ Vpp)	Media S/N (dB)
701	Co-16at% Ru	1260	37	0.0371	22.2
702	Co-16at% Ru-3at% B	1248	38	0.0367	22.1
703	Co-16at% Ru-10at% B	1140	38	0.0339	22.7
704	Co-16at% Ru-20at% B	1236	39	0.0354	22.3
705	Co-16at% Ru-23at% B	1020	33	0.0595	19.0
706	Co-30at% Ru-8at% B	1284	35	0.0376	22.7
707	Co-3at% Ru-8at% B	1164	38	0.0384	22.5
708	Co-10at% Ru-5at% Cr	1200	40	0.0389	22.4
709	Co-3at% Ru-18at% Cr-6at% B	1188	41	0.0391	21.6
710	Co-14at% Ru-5at% C	1248	37	0.0397	22.5
711	Co-14at% Ru-5at% Cr-5at% C	1260	39	0.0405	22.5
Comparative example	Co-18at% Cr-9at% Pt-6at% B	1212	33	0.0448	20.2

For the media of the sample Nos. 701 and 702

5 shown in Table 20, the crystal grain sizes of each upper magnetic layer were observed by means of a transmission electron microscope with an acceleration voltage of 200 kV. Then, the mean grain size was estimated in the following manner. First, the area of  
10 each crystal grain was calculated by using the obtained lattice image magnified two million times, and the diameter of the perfect circle having the same area as this calculated area was defined as the grain size of the crystal grain. At this step, the area in which the  
15 lattice stripes had the same orientation was regarded as one crystal grain, while the crystal grains having such a structure (bi-crystal structure) that they were adjacent to each other with their c-axes intersecting at right angles were regarded as different crystal

grains. The grain sizes were calculated from about 150 crystal grains, and the arithmetic mean thereof was taken to be regarded as the mean grain size.

[0059]

5       The mean grain size of the upper magnetic layer was 10.3 nm for the medium of the sample No. 701. In contrast, it was 9.6 nm, i.e., about 7 % microfiner, for the medium of the sample No. 702. On the other hand, for the medium of the sample No. 705 containing B  
10      in an amount of 23 at%, it was shown from the results of the X-ray diffraction measurement that the (11.0) orientation of the magnetic layer was largely deteriorated. It has been shown from the foregoing description as follows. Namely, in order to largely  
15      reduce the media noise by making fine the magnetic grain size, the B content of the lower magnetic layer is more desirably set at not less than 3 at% to not more than 20 at%.

[0060]

20       Whereas, for both the medium (sample No. 706) having a Ru content of 30 at% and the medium (sample No. 707) having a Ru content of 3 at%, the noise was low. This has indicated that it is possible to obtain a low noise medium if the Ru content of the lower magnetic  
25      layer falls within a range of 3 at% to 30 at%.

[0061]

As for the media (sample Nos. 708 and 709) in each of which the lower magnetic layer contained Cr,

the overwrite characteristic was particularly good. Whereas, for the media (sample Nos. 710 and 711) in each of which C in place of B was added to the lower magnetic layer, the media noise was slightly higher,  
5 but the output resolution was high, and a high S/N was shown. On the other hand, for the medium in which a Co-20 at% Cr-12at% Pt-6 at% B alloy was used for the lower magnetic layer of the comparative example, the overwrite characteristic was bad, and the media noise  
10 was also high.

[0062]

<Example 8>

A 35 nm-thick Ni-30at% Nb alloy layer was formed as each first underlayer, and a 10 nm-thick Cr-15at% Ti alloy layer was formed as each second underlayer. Then, as each third underlayer, a 3 nm-thick Co-34at% Cr alloy layer was formed. Subsequently, as each lower magnetic layer, the layer of Co-4at% Re, Co-8at% Re-11at% B, Co-6at% Re-5at% Cr, Co-5at% Re-5at% Cr-6at% B,  
15 Co-12at% Re-8at% C, or Co-4at% Re-4at% B-4at% C alloy layer was formed with a thickness of 2 to 6 nm. Thereafter, a 18 nm-thick Co-20at% Cr-11at% Pt-7at% B alloy layer was formed via a 0.4 nm-thick Ru intermediate layer.  
20

[0063]

Each magnetization curve was measured by applying a magnetic field in the in-plane direction, and steps have been observed in the area in which the magnetic

field is positive. This has indicated that the magnetizations of the upper magnetic layer and the lower magnetic layer are oriented in antiparallel to each other in the residual magnetization state. Table 5 21 shows the electromagnetic transfer characteristics evaluated by using the same magnetic head as that described in Example 1. Any of the media exhibited a high media S/N of 21 dB or more.

[0064]

10 Table 21

Sample No.	Lower magnetic layer	So ( $\mu$ Vpp)	OW (dB)	Nd/So ( $\mu$ Vrms/ $\mu$ Vpp)	Media S/N (dB)
801	Co-4at% Re	1358	34	0.0385	21.2
802	Co-8at% Re-11at% B	1302	35	0.0347	21.9
803	Co-6at% Re-5at% Cr	1456	37	0.0377	21.3
804	Co-5at% Re-5at% Cr-6at% B	1470	38	0.0402	21.0
805	Co-12at% Re-8at% C	1414	33	0.0413	21.1
806	Co-6at% Re-6at% Cr-8at% C	1442	33	0.0399	21.2
807	Co-4at% Re-4at% B-4at% C	1456	33	0.0403	21.3

<Example 9>

As each first underlayer, a 100 nm-thick Ni-50 at% Al alloy layer was formed, and as each second underlayer, a 25 nm-thick Cr-50 at% V alloy layer was formed. Then, the third underlayer was not provided, and each magnetic layer and each protective layer were successively deposited directly thereon. The first underlayer was formed on a 50 nm-by-50 nm basis in two separate chambers in such a manner as to be formed with a thickness of 50 nm each in respective ones of the two chambers. The substrate heating was carried out prior

to formation of the underlayer so that the substrate temperature was 280 °C. The deposition conditions for respective layers were the same as in Example 1, and the layer configuration of the magnetic layer and the  
5 Ru intermediate layer was the same as that of the medium of the sample No. 114. The X-ray diffraction measurement was carried out, and only the diffraction peak from the (10.0) plane was observed from the magnetic layer. This has indicated that it is the  
10 (10.0)-oriented medium. Further, in the magnetization curve, steps have been observed in the area in which the magnetic field is positive. This has indicated that the magnetizations of the upper magnetic layer and the lower magnetic layer are oriented in antiparallel  
15 to each other in the residual magnetization state. The coercivity, the S\*, and the Br·t were 303 kA/m, 0.70, and 4.8 T·nm, respectively, and the Ku-v/kT was 105. The electromagnetic transfer characteristics were evaluated by using the same magnetic head as in Example  
20 1. As a result, the normalized media noise was 0.0365 µVrms/µVpp, and the media S/N was 22.0 dB. Thus, such good results were obtained.

[0065]

<Example 10>

25 A NiP-plated Al-Mg alloy substrate was heated up to 220 °C. Then, as the underlayers, a 10 nm-thick Cr layer, a 20 nm-thick layer of alloy of Cr containing B in an amount of 0 to 12 at%, and a 5 nm-thick Co-37at%

Cr alloy layer were successively stacked. Subsequently, the magnetic layer and the protective layer were successively formed. As the B-containing Cr alloy, Cr-40at% Mo-2at% B, Cr-40at% Mo-4at% B, Cr-40at% Mo-6at% B,  
5 Cr-40at% Mo-8at% B, Cr-40at% Mo-10at% B, or Cr-40at% Mo-12at% B was used. As a comparative example, a medium using a Cr-40at% Mo alloy not containing B was manufactured. The layer configuration of the magnetic layer and the Ru intermediate layer was the same as  
10 that of the medium of the sample No. 214. In each of the media of this example, the Al-Mg alloy substrate is used. Therefore, the first underlayer for causing the Cr alloy to be (100)-oriented is not formed. Further, in order to ensure the compatibility between the  
15 intensive (100) orientation and the microfine crystal grains, the second underlayer made of the Cr alloy was so configured as to have a double layered structure.

[0066]

The X-ray diffraction measurement of each of the  
20 media of this example was carried out. As a result, for all the media other than the medium using the Cr-40at% Mo-12at% B underlayer, there were observed the diffraction peaks from the (100) planes of Cr and the CrMoB alloy underlayers, and intensive diffraction  
25 peaks from the (11.0) planes of the third underlayers and the magnetic layers. For the medium using the Cr-40at% Mo-12at% B underlayer, the diffraction peak from the (11.0) plane of the magnetic layer was very weak,

and an intensive (00.2) peak was observed. This has indicated that, for the medium using the Cr-40at% Mo-12at% B underlayer, the in-plane component of the c-axis is reduced.

5 [0067]

FIGS. 5(a) and 5(b) show the relationships of the B concentration of the CrMoB underlayer with the coercivity  $H_c$ , and the normalized media noise  $Nd/So$ , respectively. Herein, the normalized media noise is  
10 the value evaluated by using the same magnetic head as in Example 1. The coercivity  $H_c$  decreases with an increase in B content, and sharply decreases over a range of 10 at% to 12 at%. On the other hand, the normalized media noise  $Nd/So$  once decreases with an  
15 increase in B content, becomes minimum with respect to the B content of 6 at% to 8 at%, and then sharply increases. This has indicated as follows. Namely, in order to obtain a medium having a high coercivity of 240 kA/m or more and a low media noise of 0.04  
20  $\mu V_{rms}/\mu V_{pp}$  or less, it is desirable that the B content of the CrMoB alloy underlayer is set at 2 at% to 10 at%.

[0068]

<Example 11>

Out of the magnetic recording media 91 described  
25 in Examples 1 to 10, the media of the sample Nos. 113, 208, 213, 304, 404, 511, 609, 703, and 802, the medium shown in Example 9, and the medium using the Cr-40at% Mo-8at% B underlayer in Example 10 were selected. Then,

a magnetic storage apparatus was configured as shown in FIG. 6, which had each of these media, a driver 92 for driving the magnetic recording medium, a magnetic head 93 made up of a write element and a read element,  
5 means 94 for causing the magnetic head to perform relative movement with respect to the magnetic recording medium, and a read / write signal processing means 95 for performing the signal input to the magnetic head and output signal read-back from the  
10 magnetic head, and a station unit 96 for shelter during unloading.

[0069]

The read element of the magnetic head was made up of a magnetoresistive head. FIG. 7 is a schematic perspective view showing the configuration of the magnetic head. This head is a composite head having both the inductive head for writing and the magnetoresistive head for reading formed on a substrate 801. The writing head is made up of an upper magnetic pole 803 and a lower magnetic pole-cum-upper shield layer 804 with a coil 802 interposed therebetween. The gap length between the two magnetic poles was set at 0.14  $\mu\text{m}$ . Further, a 1.5  $\mu\text{m}$ -thick copper wire was used for the coil. The reading head was made up of a  
20 magnetoresistive sensor 805 and electrode patterns 806 on opposite sides thereof. The magnetoresistive sensor was interposed between the lower magnetic pole-cum-  
25 upper shield layer 804 and a lower shield layer 807.

The distance between the two shield layers was set at 0.10  $\mu\text{m}$ . Incidentally, in this figure, the gap layer between the magnetic poles and the gap layer between the shield layer and the magnetoresistive sensor are

5 omitted.

[0070]

FIG. 8 shows the cross sectional configuration of the magnetoresistive sensor. A signal sensing region 900 of the magnetic sensor is configured with a  
10 magnetoresistive sensor (spin-valve type read element) including a plurality of conductive magnetic layers of which mutual magnetization directions relatively change due to the external magnetic field, thereby generating a large resistance change, and conductive non-magnetic  
15 layers disposed each between the conductive magnetic layers. This magnetic sensor is so configured that on a gap layer 901, a Ta buffer layer 902, a lower magnetic layer 903, an intermediate layer 904 configured with copper, an upper magnetic layer 905, and an anti-ferromagnetic layer 906 made of a Pt-Mn  
20 alloy are successively formed. A Ni-20at% Fe alloy was used for the lower magnetic layer, and cobalt was used for the upper magnetic layer. The magnetization of the upper magnetic layer is fixed in one direction due to  
25 the exchange field from the anti-ferromagnetic layer. In contrast, the direction of the magnetization of the lower magnetic layer in contact with the upper magnetic layer via the non-magnetic layer is changed due to the

leakage field from the magnetic recording medium, so  
that the resistance change occurs. There are tapered  
regions 907 each processed in tapered form on opposite  
sides of the signal sensing region. The tapered  
5 regions are made up of permanent magnet layers 908 for  
converting the lower magnetic layer into a single  
domain, and a pair of electrodes 806 for taking a  
signal formed thereon. The permanent magnet layer is  
required to have a large coercivity and have a  
10 magnetization direction not changing with ease. For  
this reason, a Co-Cr-Pt alloy was used.

[0071]

Out of the magnetic recording media 91 described  
in Examples 1 to 8, the media of the sample Nos. 113,  
15 208, 213, 304, 404, 511, 609, 703, and 802, the medium  
shown in Example 9, and the medium using the Cr-40at%  
Mo-8at% B underlayer in Example 10 were selected. Then,  
each medium was used in combination with the head shown  
in FIG. 7 to configure the magnetic storage apparatus  
20 shown in FIG. 6. By the magnetic storage apparatus  
configured in this manner even if any of the media was  
used, it was possible to achieve a recording density of  
50 Mbit/mm<sup>2</sup> or more.

[0072]

25 In this example, there was used a magnetic head  
in which the magnetoresistive head was formed on the  
magnetic head slider having an air bearing surface rail  
area of 1.4 mm<sup>2</sup> or less and a mass of 2 mg or less. By

setting the area of the air bearing surface rail of the slider at 1.4 mm<sup>2</sup> or less, and further setting the mass at 2 mg or less, it was possible to improve the shock resistance reliability. In consequence, it was

5 possible to ensure the compatibility between the high recording density and the high shock resistance.

Accordingly, it was possible to implement a mean time between failures (MTBF) of 300,000 hours or more with a recording density of 50 Mbit/mm<sup>2</sup> or more.

10 [0073]

[Effects of the Invention]

The magnetic recording medium of the present invention has effects of reducing the media noise and improving the stability against the thermal fluctuation.

15 By using the magnetic recording medium of the present invention and the magnetoresistive head, it becomes possible to implement a magnetic storage apparatus having an areal recording density of 50 Mbit/mm<sup>2</sup> or more, and a mean time between failures of 300,000 hours or more.

20

[Brief Description of the Drawings]

[FIG. 1]

This is a graph showing a hysteresis loop of a medium of one example of the present invention;

25 [FIG. 2]

This is a schematic diagram showing one example of a cross sectional structure of a magnetic recording medium of the present invention;

[FIG. 3]

This is a schematic diagram showing the configuration of a disc formation apparatus used in the present invention;

5 [FIG. 4]

This is an enlarged view of a portion at a magnetic field of around zero of the hysteresis loop of a medium of one example of the present invention;

[FIG. 5]

10 (a) and (b) are graphs respectively showing the relationships of the coercivity, and the normalized media noise with the B content of the underlayer of a medium of one example of the present invention;

[FIG. 6]

15 This is a perspective view showing one example of a magnetic storage apparatus of the present invention;

[FIG. 7]

20 This is a perspective view showing one example of the cross sectional structure of a magnetic head in the magnetic storage apparatus of the present invention; and

[FIG. 8]

25 This is a schematic diagram showing one example of the cross sectional structure of a magnetoresistive sensor unit of the magnetic head in the magnetic storage apparatus of the present invention.

[Description of the Reference Numerals]

11: substrate

12: first underlayer

13: second underlayer                  14: third underlayer  
15: lower magnetic layer              16: intermediate layer  
17: upper magnetic layer              18: protective layer  
19: lubricant layer                    20: charging chamber

5        21: first underlayer forming chamber  
          22: heating chamber  
          23: second underlayer forming chamber  
          24: third underlayer forming chamber  
          25: lower magnetic layer forming chamber

10      26: intermediate layer forming chamber  
          27: upper magnetic layer forming chamber  
          28: protective layer forming chamber  
          28': protective layer forming chamber  
          29: discharging chamber        30: main chamber

15      91: magnetic recording media  
          92: driver for driving a magnetic recording medium  
          93: magnetic head              94: magnetic head driving means  
          95: signal processing means for recording or  
          reproducing signal

20      96: station unit for shelter during unloading  
          802: coil                    803: upper magnetic pole  
          804: lower magnetic pole-cum-upper shield layer  
          805: magnetoresistive sensor  
          806: electrode pattern      807: lower shield layer

25      900: signal sensing region  
          901: gap layer between the shield layer and the  
          magnetoresistive sensor      902: buffer layer  
          903: lower magnetic layer    904: intermediate layer

905: lower magnetic layer

906: anti-ferromagnetic layer    907: tapered region

908: permanent magnet layer

[Type of the Document] Abstract of the Disclosure

[Abstract]

[Purpose] It is an object of the present invention to provide a high reliability magnetic storage apparatus capable of performing writing and reading back of highly dense information.

5 [Solving Means]

The magnetic storage apparatus is so configured as to have a longitudinal magnetic recording medium including: a magnetic layer formed on a non-magnetic substrate via a plurality of underlayers; the magnetic layer including a lower magnetic layer containing Ru or Re in an amount of not less than 3 at% to not more than 30 at%, and Cr in an amount of not less than 0 at% to not more than 18 at%, and further containing at least one of B or C in an amount of not less than 0 at% to not more than 20 at%, and an upper magnetic layer containing Co as a main component disposed thereon via a non-magnetic intermediate layer; a driver for driving it in the recording direction; a composite magnetic head in which the read element is configured with a spin-valve type sensor; means for causing the magnetic head to perform relative movement with respect to the magnetic recording medium; and a read / write signal processing means for performing the signal input to the magnetic head and output signal read-back from the magnetic head.

10  
15  
20  
25 [Selected Figure] FIG. 2

O I P E  
JUL 20 2004  
RECEIVED  
U.S. GOVERNMENT PRINTING OFFICE

1/4

**FIG. 1**

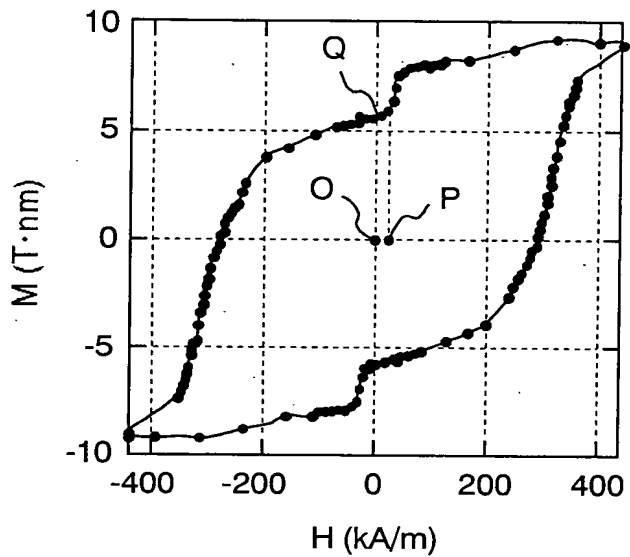
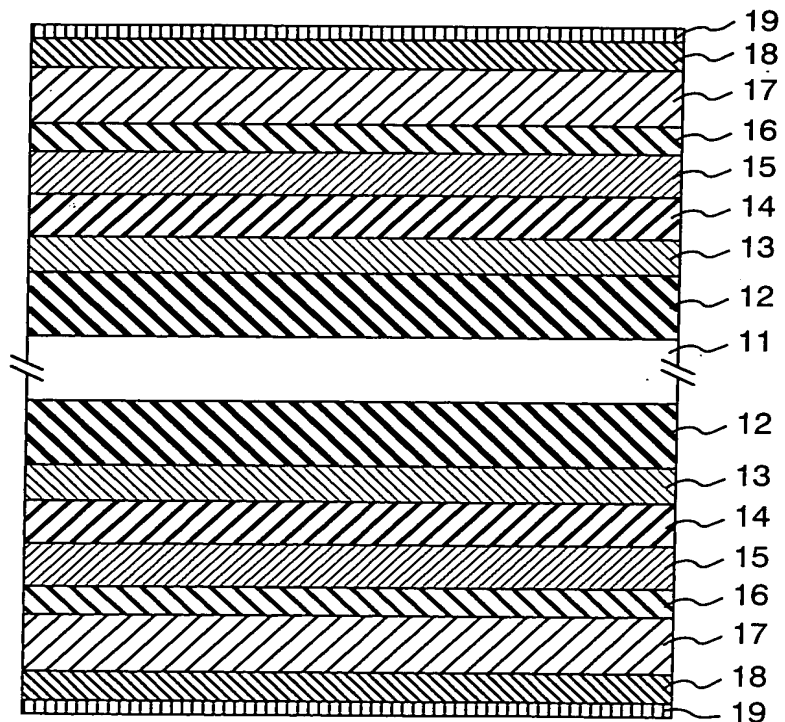


**FIG. 2**



O I P E  
JUL 20 2004  
P R I V A T E P R O P E R T Y  
O F F I C E

2/4

**FIG. 3**

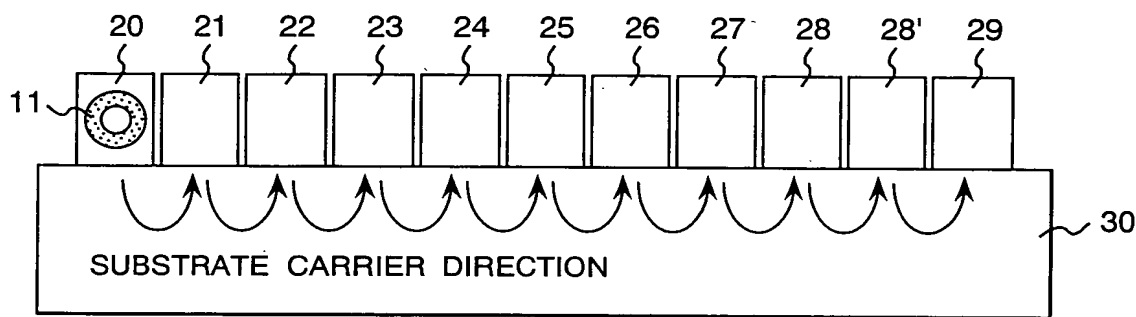
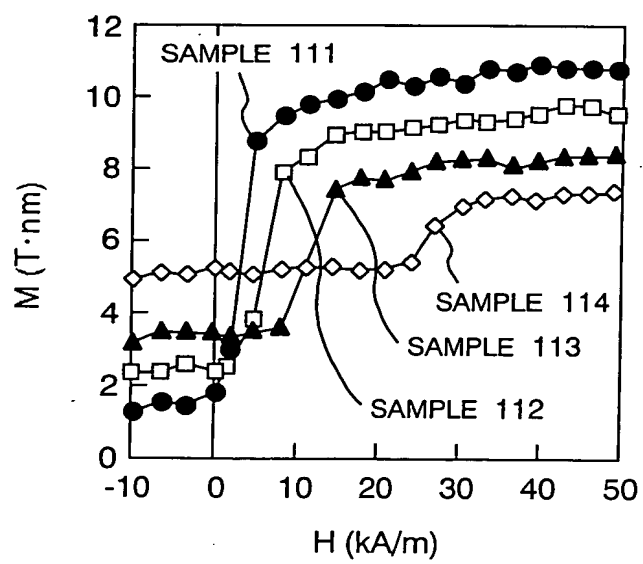


**FIG. 4**



OIPE  
JUL 20 2004  
CONFIDENTIAL

3/4

**FIG. 5a**

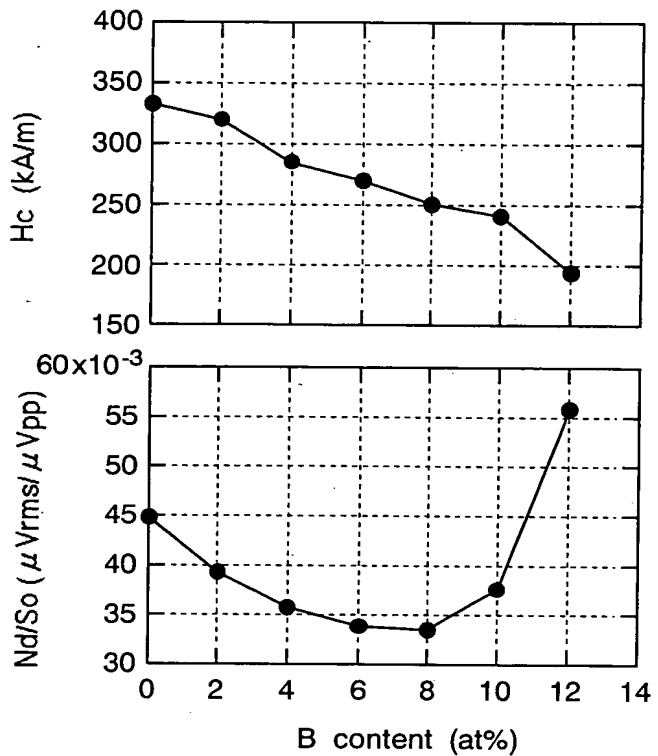


**FIG. 5b**

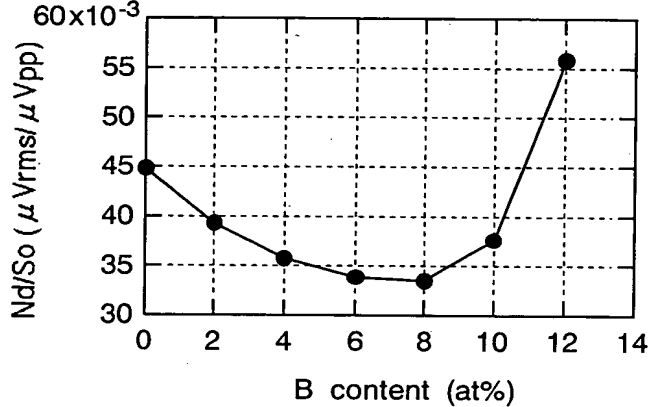
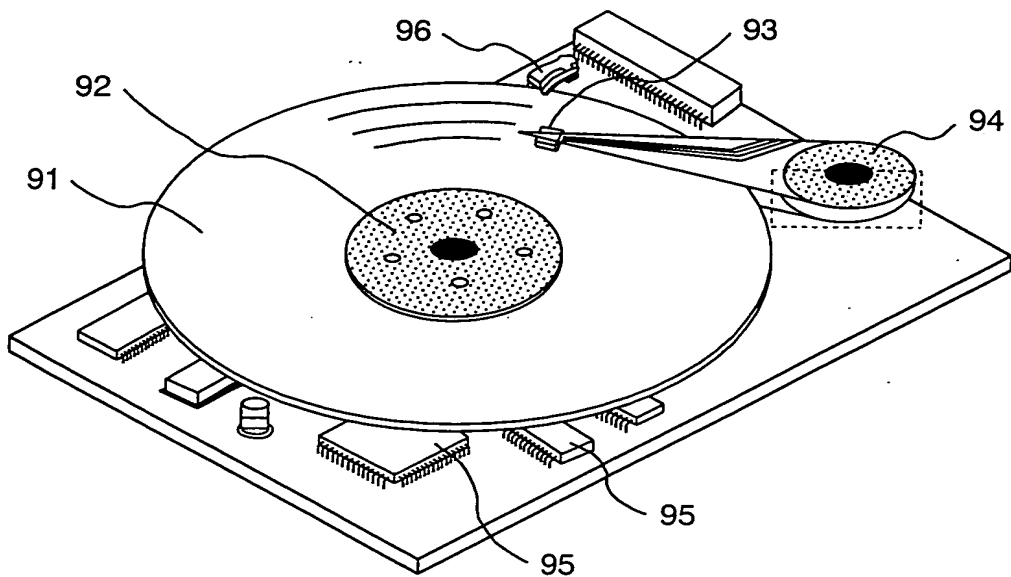


**FIG. 6**



O I P E  
JUL 20 2004  
S E C R E T

4/4

**FIG. 7**

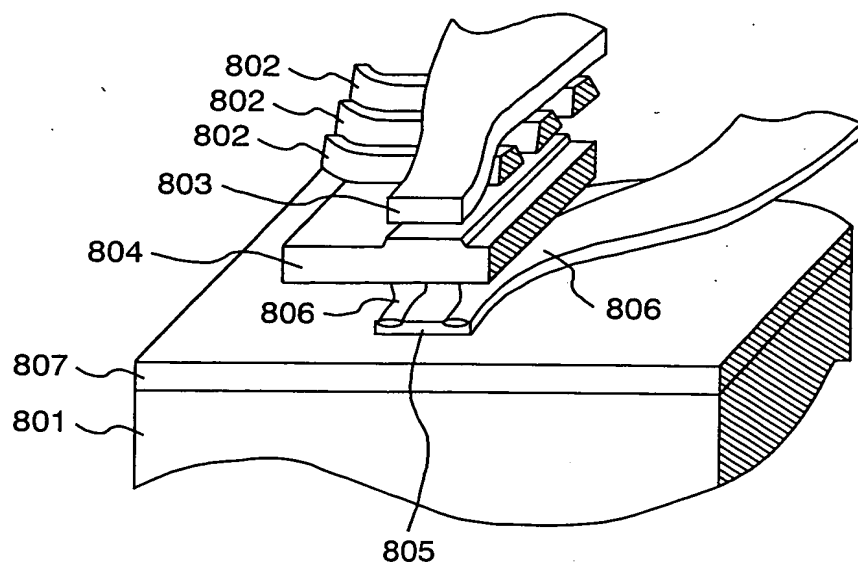


**FIG. 8**

